ISSN : 0974 - 7524 Volume 9 Issue 6

Physical CHEMISTRY
An Indian Journal

Full Paper

PCAIJ, 9(6), 2014 [195-204]

Theoretical study of the effects of structure and localization of the π electron clouds of single-walled carbon nanotubes on the π-π stacking interactions

Pouya Karimi*, Mahmoud Sanchooli
Department of Chemistry, Faculty of Science, University of Zabol, Zabol, (IRAN)
E-mail : pouyasman@gmail.com

ABSTRACT

An armchair (4,4) graphene sheet has been rolled up to build single-walled carbon nanotube fragments (SWCNTFs) by computational quantum chemistry methods. Noncovalent π-π stacking interactions of the benzene molecule with the central rings of SWCNTFs have been investigated. The binding energies of the π-π stacked benzene-SWCNTF complexes versus R (true strain parameter) change in three brands. Structural parameters, electron charge density values at the bond and ring critical points of all SWCNTFs and π-π stacked complexes were studied. Also, effects of aromaticity and charge transfer (CT) on the binding energies were gauged. Results indicate that partially localization of the π electron clouds of SWCNTFs enhances strength of the π-π stacking interactions in some cases. Thus, changing the π electron clouds of SWCNTs improves noncovalent functionalization of these materials through the π-π stacking interactions, which has an important role in biomedical applications such as in cancer therapy.

KEYWORDS

π-π stacking;
Graphene sheet;
Electron charge density;
Aromaticity;
π electron cloud.

INTRODUCTION

Carbon Nanotubes (CNTs)[1] are a new type of materials which consist of one [single-walled carbon Nanotubes (SWCNTs)] to tens of coaxial tubes [multi-walled carbon Nanotubes (MWCNTs)]. SWCNTs and MWCNTs have the diameters range from 0.4 to 6.0 and 2.0 to 50.0 nm, respectively.

Diameter of CNTs is an important parameter that controls the unique physical, mechanical and chemical properties of them. Carbon atoms of the CNT surface have SP2-hybridization. The p-orbital electrons of the graphene sheet arrange in band valence (π) and conduction (π*) bands[2]. When graphene sheet is rolled up to the cylindrical form of SWCNT, its π and π* electron clouds change which causes partial σ- π hybridization[3]. Thus, the electron charge density around a small diameter SWCNT is dispersed, while a large diameter SWCNT has confined electron charge density at the atomic core position.

CNTs have significantly larger length to diameter ratio than any other material[4]. SWCNs with different diameters and therefore variable surface area are good beds for interactions of biomolecules. Surfaces of small

diameter CNTs are polarized, but large diameter CNTs have more hydrophobic surfaces[5].

The electronic structure of SWCNTs is related to the tube diameter (d) and depends on the pair (n,m) which demonstrates the number of unit vectors in the graphene sheet lattice. This electronic structure changes upon interactions of proteins or DNA with surfaces of SWCNTs.

Electronic properties of SWCNTs make them useful biosensors[6,7]. The unique properties of CNTs make them capable of drug delivery for treatment of various diseases[8]. For example, CNTs act as potent drug delivery vehicles in cancer therapy[9]. Indeed, CNTs can be used as multifunctional biological transporters and near-infrared agents for selective devastation of cancer cells[10].

CNTs have nano scale dimensions and deliver smaller doses of drugs in the body which results in lower side effects. Therefore, efficiency of CNTs in disease cell targeting improves remarkably[11].

CNTs act as molecular transporters for walled plant cells and are able to penetrate cell membranes. This motif has fundamental importance for plant intracellular labeling and imaging, genetic transformation and understanding plant cell biology[12].

CNTs have a very low solubility in aqueous solutions and this matter is a major barrier for a variety of applications. Surface functionalization of CNTs by covalent or noncovalent interactions is an effort to increase solubility of these materials in various solvents[13-17].

Functionalization of SWCNTs with (R-) oxycarbonyl Nitrenes have been experienced by M. Holzinger et al.[18]. They showed that this sidewall functionalization allows the covalent binding of alkyl chains, aromatic groups, dendimers, crown ethers and oligoethylene glycol units to SWCNTs and leads to a significant increment of solubility in organic solvents.

Polar functional groups increase interactions of CNTs with charged polypeptides[19,20]. Functionalized SWCNTs are able to carry small interfering RNA into cells. These materials can become useful in the therapeutic strategy for chronic myelogenous leukemia cells[21].

Unlike covalent modification of SWCNTs, which partly deforms the electronic and structural properties of these materials, noncovalent modifications improve solubility of them. Indeed, geometric, electronic and mechanical properties of SWCNTs preserve through noncovalent modifications.

In several published works, functionalization of SWCNTs with biomolecules and their biomedical applications have been reported[13,22-23]. Noncovalent interactions of biomacromolecules with the surface of SWCNTs have considered recently in both aqueous and organic solvents[24-29].

Noncovalent functionalization of SWCNTs via π-π stacking forces exerts minor disorderliness on the carbon nanotube electronic network[24]. Functionalized SWCNTs have high tendency to cross cell membranes and are useful for the delivery of therapeutically active molecules[30].

Anindya Das et al. have utilized the ab initio Hartree-Fock method together with the classical force field calculation to estimate the binding energy of nucleobases with (5,5) SWCNTs[31].

Stepan G. Stepanian et al. have studied interactions between Nucleic Acid Bases (NABs) and SWCNTs[32]. They used MP2 method for optimization of structures and also evaluated ability of various DFT methods in predicting the optimized structures and binding energy values. They showed that M05-2X functional is capable of correctly predicting structures and binding energies, but M05, MPWB1K and MPW1B95 density functionals are only capable of correctly predicting the structure of SWCNT-NAB complexes.

Noncovalent π-π stacking and cooperative CH···π/NH···π interactions of the cytosine molecule with SWCNTs have been investigated by Wang and Bu[33]. They showed that electron correlation is a dominant source for π-π stacked conformations and electrostatic attractions have major roles on the stability of CH…π and NH…π complexes.

Tapas Kar et al. have employed the MP2 method to evaluate the binding energy of the benzene and naphthalene molecules at the outer surfaces of different nanotubes[34]. They showed that configuration which the benzene molecule lays on the top of a CP%C double bond of SWCNT is the most stable structure.

Wang et al. have studied adsorption of nine tripeptides on SWCNTs with MPWB1K and MP2 methods[35]. They revealed that the aromatic groups of proteins play important role in functionalization of

SWCNTs, and complexes with aromatic residues have the highest electron correlation effects.

Some authors investigated adsorption of the drug isoniazid onto carbon nanotubes using DFT calculations[36]. Also, N. C. Deka et al. revealed preferential site selectivity for adsorption of drug isoniazid onto different carbon nanotubes[37].

The binding energies of interaction of 2-methylheptylisonicotinate antitubercular drug onto carbon nanotubes have been reported using DFT-PW91/DNP calculations[38]. Also, pyrazinamide adsorption onto covalently functionalized (5,5) single walled carbon nanotube has been investigated using theoretical studies[39].

Because functionalized-SWCNTs have biomedical applications, such as in cancer therapy, it is necessary to understand effects of various factors which control functionalization of SWCNTs. It seems that, delocalization and localization of the π electron clouds of SWCNTs to be important in noncovalent functionalization of these materials through the π-π stacking interactions.

In this work, an (4,4) armchair graphene sheet has been rolled up by computational quantum chemistry methods to build single-walled carbon nanotube fragments (SWCNTFs). These SWCNTFs have the same number of atoms and represent parts of SWCNTs with different outer diameters. The π-π stacking interactions of the benzene molecule with the central rings of SWCNTFs were investigated. Structural parameters, electron charge density values at the bond and ring critical points (BCP and RCP) of all SWCNTFs and π-π stacked benzene-SWCNTF complexes were studied. Also, effects of aromaticity and charge transfer (CT) were gauged to determine roles of delocalization and localization of the π electron clouds of SWCNTs on the π-π stacking binding energies. Results highlight the role of partially localization of the π electron clouds of SWCNTs in enhancement of the π-π stacking binding energies in some cases.

COMPUTATIONAL METHODS

Structures of all monomers and complexes were optimized with Gaussian09 program package[40] at the M05-2X/6-31G (d) level of theory. The second-order Møller-Plesset perturbational method (MP2) usually overestimate binding energy (|ΔE|) values and is not adequate for evaluation of the π–π stacking binding energies. The DFT methods are useful for studying the biological systems, but the B3LYP method fails for dispersion interactions and can't describe the π–π stacking interactions. However, Stepan G. Stepanian et al. have studied interactions between Nucleic Acid Bases (NABs) and SWCNTs[32]. They showed that the M05-2X functional is capable of correctly predicting structures and binding energies of SWCNT-NAB complexes. Indeed, Zhao and Truhlar proposed that hybrid meta-GGA M05-2X functional has good performance for computing π–π stacking binding energies[41]. They showed that the M05-2X functional compensate the deficiencies of other hybrid functionals by incorporating an improved treatment of spin kinetic energy density in both the exchange and correlation functionals.

The interaction energy of each complex was calculated as difference between energy of binary complex and constituting monomers:

$$\Delta E = E_{benzene\text{-}SWCNTF} - (E_{benzene} + E_{SWCNTF}) \quad (1)$$

Therefore, the binding energy of each complex was considered as absolute value of interaction energy (|ΔE|).

The binding energies were calculated with correction for the basis set superposition error (BSSE) using the Boys-Bernardi counterpoise technique[42]. The topological properties of electron charge density have been calculated by the AIM method on the wave functions obtained at the M05-2X/6-31g (d) level of theory using AIM2000 program[43]. Atomic net charges have been calculated using ChelpG schemes[44] at the above mentioned level. The diamagnetic and paramagnetic effects of ring currents related to aromaticity and antiaromaticity can be evaluated by nucleus independent chemical shift (NICS)[45,46] criterion. The NMR calculations have been performed at the M05-2X/6-31g (d) level of theory using gauge independent atomic orbital (GIAO) method[47].

RESULTS AND DISCUSSION

Structural parameters and energy data

An armchair (4,4) graphene sheet has been constructed using HyperChem 7.1 software[48]. This

graphene sheet is shown in the Scheme 1. To generate SWCNTFs, potential energy surface (PES) relaxed scans were performed. In fact, distances of terminal hydrogens of the graphene sheet were fixed as redundant coordinates. These distances were reduced by 10 Å during 100 step-by-step full optimizations. Thus, each SWCNTF has a true strain parameter (R) which can be estimated as below:

$$R = Ln (r_0/r) \quad (2)$$

In this equation, r_0 and r is the distances between terminal hydrogens of the graphene sheet and SWCNTFs, respectively. Also, terminal C-H bond lengths of the graphene sheet and SWCNTFs were kept constant during 100 step-by-step full optimizations.

The π-π stacking interactions of the benzene molecule with the central rings of SWCNTFs have gauged.

Typical structures of the π-π stacked benzene-graphene sheet and one case of the π-π stacked benzene-SWCNTF complexes are shown in Scheme 2.

Binding energies of all π-π stacked benzene-SWCNTF complexes versus R are depicted in Figure 1. As can be seen, |ΔE| values vary in three brands. In fact, the three brands show decrement or increment of the binding energies with increment of R. In the first brand (■), increment of R is accompanied by decrement of ΔE values with a sharp slope. In the second brand (▲), increment of R is accompanied by decrement of |ΔE| values. Finally, in the third brand (×), increment of R is accompanied by increment of |ΔE| values with a mild slope.

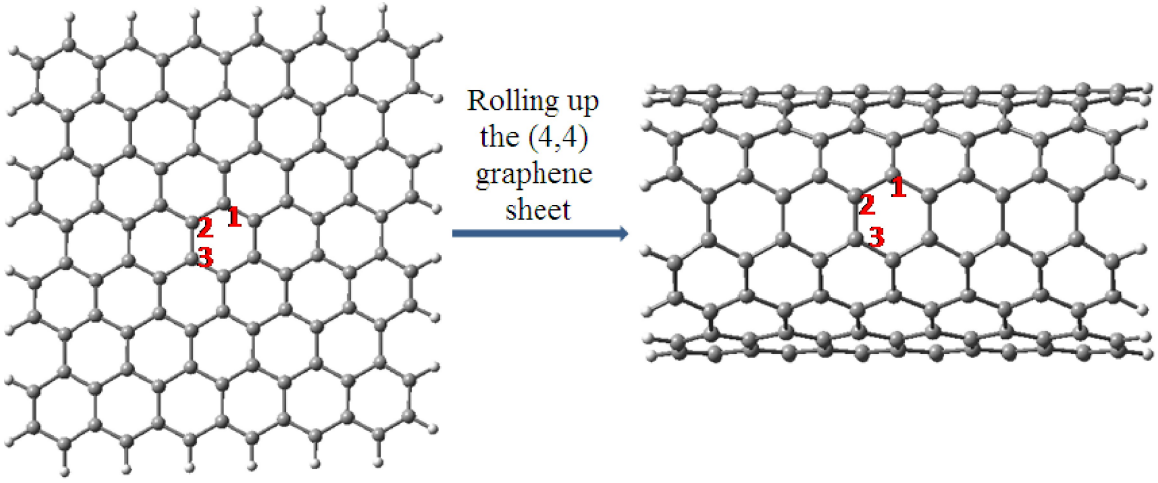

Scheme 1 : Rolling up the (4,4) graphene sheet to build SWCNTFs

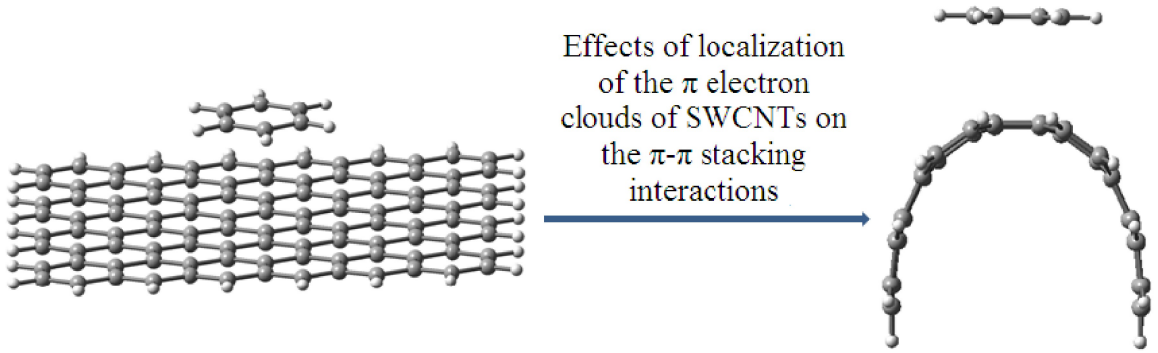

Scheme 2 : Typical structures of the π-π stacked benzene-graphene sheet and one case of the π-π stacked benzene-SWCNTF complexes

To explain this binding energy changes, the most important structural parameters of all complexes were studied. Results show that the π-π stacking interactions of the benzene molecule with the central rings of SWCNTFs lead to decrement of bond lengths of these rings (C1-C2 or C2-C3 bonds in Scheme 1). However, unlike covalent functionalization, these interactions don't change surfaces of SWCNTFs.

In Figure 2, |ΔE| values against the C1-C2 bond lengths of all π-π stacked benzene-SWCNTF com-

plexes are demonstrated.

As can be observed, in the first brand (■), decrement of |ΔE| values initially is accompanied by decrement of the C1-C2 bond lengths. In these complexes the benzene molecule interacts with the graphene sheet and some SWCNTFs with large outer diameters. In fact, rolling up the planar graphene sheet leads to decrement of |ΔE| values. Then, few complexes are observed which decrement of |ΔE| values isn't accompanied by changes of the C1-C2 bond lengths. Finally, decrement of |ΔE| values is accompanied by increment of the C1-C2 bond lengths. In the second brand (▲), decrement of |ΔE| values is accompanied by increment of the C1-C2 bond lengths. On the other hand, in the third brand (×), decrement of |ΔE| values is followed by decrement of the C1-C2 bond lengths. Results show that rolling up the graphene sheet initially leads to decrement of the C1-C2 bond lengths. However, this decrement in the C1-C2 bond lengths continues to a minimum and then increment of the C1-C2 bond lengths occurs. As was said, the π-π stacking interactions of the benzene molecule with the central rings of SWCNTFs lead to slightly decrement of the C1-C2 bond lengths. In fact, rolling up the graphene sheet leads to a change in the π electron clouds of SWCNTFs. This change influences the π-π stacking interactions of the benzene molecule with SWCNTFs.

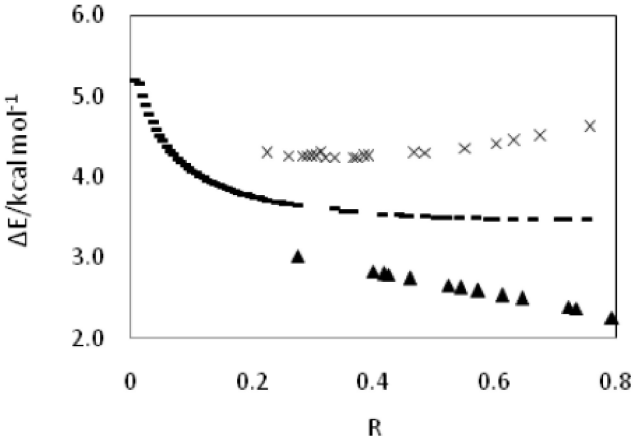

Figure 1 : The binding energies of the π-π stacked benzene-SWCNTF complexes versus rolling up parameter for the first (■), second (▲), and third (×) brands

The vertical equilibrium distance between the benzene molecule and each SWCNTF is denoted as Rc-c. Investigation of the correlations between the Rc-c and ΔE values may help to find reason of these variations in the |ΔE| values. These correlations are shown in Figure 3 for all complexes.

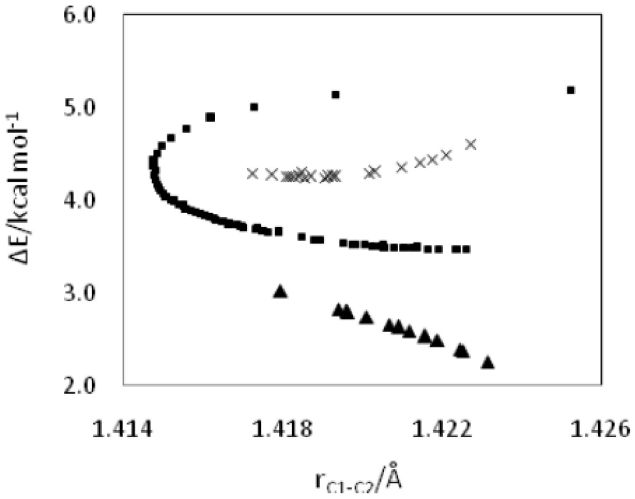

Figure 2 : The binding energies of the π-π stacked benzene-SWCNTF complexes versus C1-C2 bond lengths for the first (■), second (▲), and third (×) brands

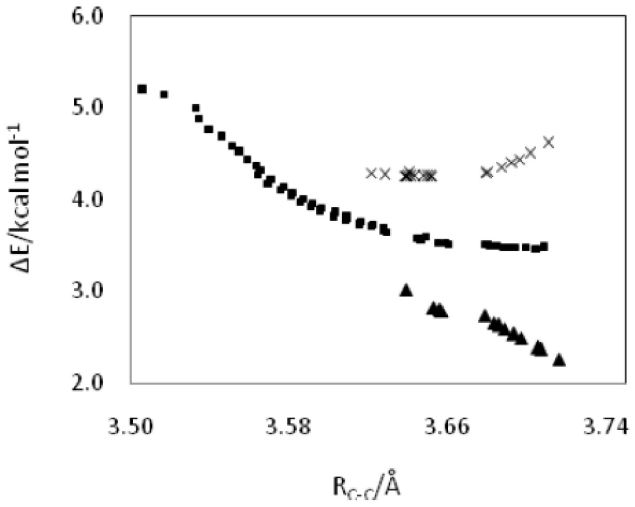

Figure 3 : The binding energies of the π-π stacked benzene-SWCNTF complexes against vertical distance between the benzene molecule and SWCNTFs for the first (■), second (▲), and third (×) brands

As can be seen, in the first (■) and second (▲) brands, decrement of binding energies is accompanied by increment of Rc-c values which is a reasonable behavior. On the other hand, in the third brand (×), complexes with the larger Rc-c values have the higher binding energies. Indeed, increment of the |ΔE| values in this brand is accompanied by increment of the C1-C2 bond lengths. These increases in the C1-C2 bond lengths imply that hyper conjugation effects diminish in these bonds which arise from lower overlap between p orbitals. In fact, π- electrons are somewhat localized in

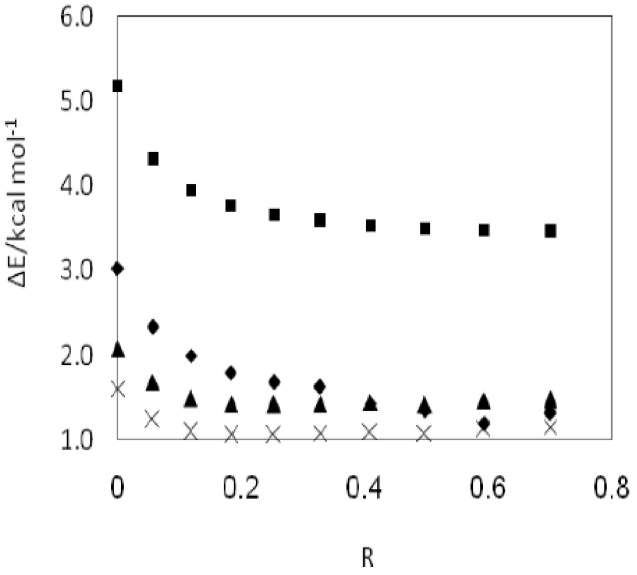

Figure 4 : The binding energies of the π-π stacked benzene-SWCNTF complexes obtained from the M05-2X (■), BSSE corrected M05-2X (♦), MPWB1K (▲), and MPW1B95 (×) methods

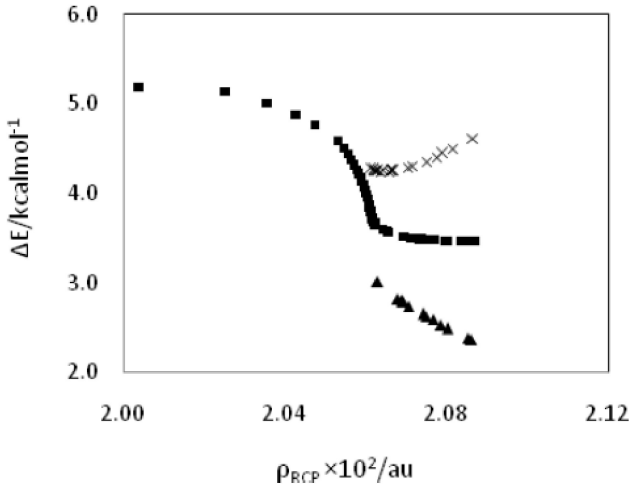

Figure 5 : The binding energies versus ρ_{RCP} values of the π-π stacked benzene-SWCNTF complexes for the first (■), second (▲), and third (×) brands

this case. Therefore, increment of the |ΔE| values which is accompanied by increment of Rc-c values can be related to the interactions of the delocalized π electron cloud of the benzene molecule and partially localized π electron clouds of SWCNTFs. This finding indicates that strength of the π-π stacking interactions on SWCNTs can be controlled by effects of delocalization and localization of the π electrons.

In accord with Koopmans theorem[49], ionization energy (I) and electron affinity (A) can be considered as $-E_{HOMO}$ and $-E_{LUMO}$ (E_{HOMO} and E_{LUMO} are highest occupied molecular orbital and lowest unoccupied molecular orbital energies, respectively). On the basis of Mulliken theory[50], tendency of a species to liberate electron at its ground state is considered as electron chemical potential which can be evaluated as below:

$$\mu = -(I + A)/2 \quad (3)$$

Results reveal that increment of R leads to decrement of EHOMO and ELUMO values of SWCNTFs. Indeed, E_{HOMO} and E_{LUMO} values of the π-π stacked benzene-SWCNTF complexes are lower than the graphene sheet and SWCNTFs. Thus, functionalization of SWCNTs through the π-π stacking interactions increases tendency of these materials to liberate electrons.

To compare binding energy values which obtained from other theoretical functionals with the M052X method, single point energy calculations have been performed on some optimized π-π stacked benzene-SWCNTF complexes by MPWB1K and MPW1B95 methods in conjunction with the 6-31G (d) basis set. As can be seen in Figure 4 the M052X method gives larger binding energies than the MPWB1K and MPW1B95 methods. Also, BSSE corrected binding energies for the some optimized π-π stacked benzene-SWCNTF complexes are shown in this Figure.

AIM analysis

To interpret changes of the binding energy values with R in the π-π stacked benzene-SWCNTF complexes, AIM calculations have been performed on the wave functions obtained at the M05/2X 6-31G (d) level of theory. Electron charge density values at the bond critical points (ρ_{BCP}) of all monomers and complexes confirm the structural parameters. Formation of the π-π stacked benzene-SWCNTF complexes leads to enhancement of the electron charge density values at the ring critical points (ρ_{RCP}) of the central ring (ring A) of the graphene sheet and SWCNTFs.

Results indicate that rolling up the graphene sheet leads to enhancement of the electron charge density values at the central rings of SWCNTFs. Indeed, increment of R leads to increment of ρ_{RCP} values at the central ring of the π-π stacked benzene-SWCNTF complexes. In Figure 5, binding energies versus the ρ_{RCP} values of the π-π stacked benzene-SWCNTF complexes are demonstrated. As can be seen, in the first

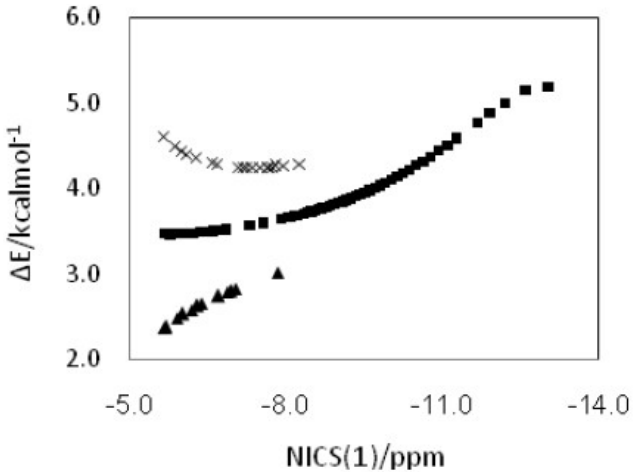

Figure 6 : The binding energies of the π-π stacked benzene-SWCNTF complexes versus NICS(1) values at the central rings of the graphene sheet and SWCNTFs for the first (■), second (▲), and third (×) brands

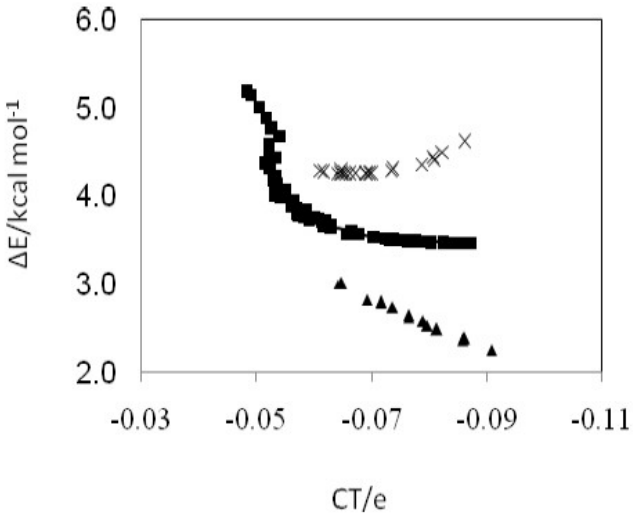

Figure 7 : The binding energies of the π-π stacked benzene-SWCNTF complexes against charge transfer for the first (■), second (▲), and third (×) brands

(■) and second (▲) brands, increment of the ρ_{RCP} values goes along with decrement of binding energies, but in the third brand (×) different behavior is observed. In this brand, increment of the ρ_{RCP} values is accompanied by increment of binding energies.

Comparison of Figure 5 and Figure 3 indicates that the ρ_{RCP} values influence the vertical equilibrium distances between the benzene molecule and SWCNTFs. In fact, rolling up the graphene sheet alters the π electron clouds and structures of SWCNTFs.

In the first (■) and second (▲) brands, delocalized π electron cloud of the benzene molecule interacts with the delocalized π electron clouds of SWCNTFs. In these cases, increment of the ρ_{RCP} values leads to decrement of binding energies. Accordingly, Rc-c values are increased. In contrast, in the third brand (×), increment of the ρ_{RCP} values is accompanied by increment of binding energies and Rc-c values. In fact, in this case delocalized π electron cloud of the benzene molecule interacts with the partially localized π electron clouds of SWCNTFs. It seems that, increment of the electron charge density values at the central rings of SWCNTFs have a repulsive effect on the interacting rings and leads to higher Rc-c values. This finding highlights the role of partially localization of the π electrons of SWCNTs in enhancement of the π-π stacking binding energies. Bloom and Wheeler have reported effects of localization of the π electrons on the binding energies of π-π stacked complexes[51]. These authors indicated that the monomer aromaticity is not necessary in aromatic interactions in some cases and localized π electrons enhance the π-π stacking binding energies. Therefore, altering the π electron clouds of SWCNTs can be important in improvement of the noncovalent functionalization of these materials through the π-π stacking interactions, which has an important role in biomedical applications such as in cancer therapy.

NMR calculations

The NMR calculations have been performed at the M05-2X/6-31g (d) level of theory using the GIAO method[47]. The NICS (0) and NICS (1) values at the central rings of the graphene sheet and SWCNTFs were evaluated. Results show that rolling up the graphene sheet leads to decrement of these values. In fact, rolling up the graphene sheet leads to a change in the π electron clouds of SWCNTFs. The NICS (0) values reveal effects of sigma-bonds at rings, while NICS (1) ones reflect π-bond effects at rings. Therefore, NICS (1) is a better criterion than NICS (0) and represents the π-aromaticity at rings.

The binding energies of the π-π stacked benzene-SWCNTF complexes versus NICS (1) values at the central ring of the graphene sheet and SWCNTFs are shown in Figure 6. As can be seen, in the first (■) and second (▲) brands, decrement of the NICS (1) values is accompanied by decrement of binding energies. As was said, in these cases delocalization of the π electron clouds of SWCNTFs (which is related to the π-aro-

maticity) is significant. In fact, more delocalized π electron clouds of SWCNTFs leads to the larger binding energies. In contrast, in the third brand (×) different behavior is observed. In this case, decrement of the NICS (1) values leads to increment of binding energies. Thus, partially localization of the π electron clouds of SWCNTFs (which is related to the less π-aromaticity) is an important factor which enhances the π-π stacking binding energies in some cases. This consequence is consistent with the result of AIM analysis and accentuates the role of partially localization of the π electrons in augmentation of the π-π stacking binding energies.

Charge transfer analysis

To understand effects of charge transfer in the π-π stacked benzene-SWCNTF complexes, atomic charges in the graphene sheet, SWCNTFs and all complexes have been calculated using the ChelpG Scheme[44]. Results indicate that formation of the π-π stacked benzene-SWCNTF complexes leads to increment of total negative charge on the benzene molecule. Consequently, charge transfer (CT) direction in these complexes is from the graphene sheet and SWCNTFs to the benzene molecule (the graphene sheet or SWCNTFs →benzene). The magnitude of this charge transfer is in the range of -0.048 – -0.091 e. The binding energies versus CT in the mentioned complexes are demonstrated in Figure 7.

As can be observed, changes of binding energies with CT are similar to the changes of these values with R (see Figure 1). Therefore, different response of SWCNTFs to the π-π stacking interactions, which generates three brands for changes of binding energy with R, can be interpreted on the basis of charge transfer effects in the π-π stacked benzene-SWCNTF complexes.

In the first (■) and second (▲) brands, increment of CT goes along with decrement of binding energies. Thus, CT isn't main factor for enhancement of the π-π stacking binding energies in these complexes. As previously was said, in these complexes larger binding energies arise from interactions between delocalized π electron cloud of the benzene molecule and more delocalized π electron clouds of SWCNTFs. Therefore, more delocalized π electron clouds of SWCNTFs leads to the less CT to the benzene molecule. On the other hand, in the third brand (×) increment of CT is accompanied by increment of the binding energies. In this case larger binding energies arise from interactions between delocalized π electron cloud of the benzene molecule and partially localized π electron clouds of SWCNTFs. Thus, in this case partially localization of the π electrons allows the less CT to the benzene molecule which enhances the π-π stacking binding energies.

As a result, strength of the π-π stacking interactions on SWCNTs is controlled by several factors, such as properties of the π electron clouds of interacting molecules, aromaticity, delocalization and localization of the π electron clouds of SWCNTs and charge transfer effects.

CONCLUSIONS

An armchair (4,4) graphene sheet was rolled up by computational quantum chemistry methods to build single-walled carbon nanotube fragments (SWCNTFs). Noncovalent π-π stacking interactions of the benzene molecule with the central rings of these SWCNTFs have been investigated.

Binding energies of the π-π stacked benzene-SWCNTF complexes versus R values vary in three brands.

Rolling up the graphene sheet leads to a change in the π electron clouds of SWCNTFs and results in different π-π stacking binding energies with benzene.

Strength of the π-π stacking interactions on SWCNTs can be controlled by effects of delocalization and localization of the π electrons.

Noncovalent functionalization through the π-π stacking interaction increases tendency of SWCNTs to liberate electrons.

Rolling up the graphene sheet leads to enhancement of the electron charge density values at the central rings of SWCNTFs.

Rolling up the graphene sheet leads to decrement of the NICS (0) and NICS (1) values at the central rings of SWCNTFs.

In some π-π stacked benzene-SWCNTF complexes, delocalization of the π electron clouds of SWCNTFs is significant and leads to increment of the π-π stacking binding energies. In contrast, in some cases partially localization of the π electron clouds of

SWCNTFs is an important factor which enhances the π-π stacking binding energies.

Charge transfer direction in the π-π stacked benzene-SWCNTF complexes is from the graphene sheet or SWCNTFs to the benzene molecule and magnitude of this charge is in the range of -0.048 – -0.091 e. Different response of SWCNTFs to the π-π stacking interactions can be interpreted on the basis of charge transfer effects in the π-π stacked benzene-SWCNTF complexes.

Altering the π electron clouds of SWCNTs can be important in improvement of the noncovalent functionalization of these materials through the π-π stacking interactions and has a vital role in biomedical applications such as in cancer therapy.

ACKNOWLEDGMENT

We thank the university of Sistan & Baluchestan for financial supports and Computational Quantum Chemistry Laboratory for computational facilities.

REFERENCES

[1] D.Tasis, N.Tagmatarchis, A.Bianco, M.Prato; J.Chem.Rev., **106**, 1105 **(2006)**.
[2] G.S.Painter, D.E.Ellis; J.Phys.Rev.B, **1**, 4747 **(1970)**.
[3] X.Blase, L.X.Benedict, E.L.Shirley S.G.Louie; J.Phys.Rev.Lett., **72**, 1878 **(1994)**.
[4] X.Wang, Q.Li, J.Xie, Zh.Jin, J.Wang, Y.Li, K.Jiang, Sh.Fan; J.Nano Lett., **9**, 3137 **(2009)**.
[5] M.A.Jie, J.N.Wang, C.J.Tsai, R.Nussinov, M.A.Buyong; Front.J.Mater.Sci.China., **4**, 17 **(2010)**.
[6] Y.Y.Wang, X.Wang, B.Wu, B.Wu, Z.Zhao, F.Yin, S.Li, X.Qin, Q.Chen; J.Sensors and Actuators B: Chemical, **130**, 809 **(2008)**.
[7] J.Tkac, J.W.Whittaker, T.Ruzgas; J.Biosensors and Bioelectronics, **22**, 1820 **(2007)**.
[8] A.Bianco, K.Kostarelos, M.Prato; J.Current Opinion in Biotechnology, **9**, 674 **(2005)**.
[9] C.Srinivasan; J.Current Science, **94**, 300 **(2008)**.
[10] N.W.S.Kam, M.O'Connell, J.Wisdom, A.H.Dai; PNAS, **102**, 11600 **(2005)**.
[11] P.J.F.Harris; Carbon nanotube science, Synthesis, Properties and Applications. Cambridge University Press, Cambridge, **(2009)**.
[12] O.Liu, B.Chen, O.Wang, X.Shi, Z.Xiao, J.Lin X.Fang; J.Nanoletters., **9**, 1007 **(2009)**.
[13] S.Kang, M.Pinault, L.D.Pfefferle, M.Elimelech; J.Langmuir., **23**, 8670 **(2007)**.
[14] Y.Lin, S.Taylor, H.P.Li, K.A.S.Fernando, L.W.Qu, W.Wang, L.R.Gu, B.Zhou, Y.P.Sun; J.Mater. Chem., **14**, 527 **(2004)**.
[15] A.Star, Y.Liu, K.Grant, L.Ridvan, J.F.Stoddart, D.W.Steuerman, M.R.Diehl, A.Boukai, J.R.Heath; J.Macromolecules., **36**, 553 **(2003)**.
[16] Y.Lin, L.F.Allard, Y.P.Sun; J.Phys.Chem.B, **108**, 3760 **(2004)**.
[17] W.Huang, S.Taylor, K.Fu, Y.Lin, D.Zhang, T.W.Hanks, A.M.Rao, Y.P.Sun; J.Nano Lett., **2**, 311 **(2002)**.
[18] H.Michael, A.Juergen W.Paul, G.Ralf, L.Lothar, H.Frank, K.Manfred, H.Andreas; J.Am.Chem.Soc., **125**, 8566 **(2003)**.
[19] X.Li, W.Chen, Q.Zhan, L.Dai, L.Sowards, M.Pender, R.R.Naik; J.Phys.Chem.B, **110**, 12621 **(2006)**.
[20] V.Z.Poenitzsch, D.C.Winters, H.Xie, G.R.Dieckmann, A.B.Dalton, I.H.Musselman; J.Am.Chem.Soc., **129**, 14724 **(2007)**.
[21] X.Wang, J.Ren, X.Qu; J.Chem.Med.Chem., **3**, 940 **(2008)**.
[22] A.Bianco, K.Kostarelos, M.Prato; J.Curr.Opin. Chem.Biol., **9**, 674 **(2005)**.
[23] A.Bianco, K.Kostarelos, C.D.Partidos, M.Prato; J.Chem.Commun., **5**, 571 **(2005)**.
[24] R.J.Chen, Y. Zhang, D.Wang, H.Dai; J.Am.Chem. Soc., **123**, 3838 **(2001)**.
[25] O.K.Kim, J.Je, J.W.Baldwin, S.Kooi, P. E.Pehrsson, L.J.Buckley; J.Am.Chem.Soc., **125**, 4426 **(2003)**.
[26] P.Barone, M.S.Strano; Angew.Chem., Int.Ed., **45**, 8138 **(2006)**.
[27] A.Star, D.W.Steuerman, J.R.Heath, J.F.Stoddart; Angew.Chem., Int.Ed., **41**, 2508 **(2002)**.
[28] A.Ishibashi, N.Nakashima; J.Chemistry, **12**, **(2006)**.
[29] P.Goodwin, S.M.Tabakman, K.Welsher, S.P.Sherlock, G.Prencipe, H.Dai; J.Am.Chem.Soc., **131**, 289 **(2009)**.
[30] L.Lacerda, V.Raffa, M.Prato, A.Bianco, K.Kostarelos; J.Nano Today., **2**, 38 **(2007)**.
[31] D.Anindya, A.K.Sood, K.M.Prabal, D.Mili, R.Varadarajan, C.N.R.Rao; J.Chem.Phys.Lett., **453**, 266 **(2008)**.
[32] G.S.Stepan, V.K.Maksym, Y.G.Alexander, A.K.Victor, L.Adamowicz; J.Phys.Chem.A, **113**,

3621 **(2009)**.
[33] W.Yixuan, B.Yuxiang; J.Phys.Chem.B, **111**, 6520 **(2007)**.
[34] K.Tapas, F.B.Holger, S.Steve, K.R.Ajit; J.Phys. Chem.C, **112**, 20070 **(2008)**.
[35] W.Yixuan, A.Hongqi; J.Phys.Chem.B, **113**, 9620 **(2009)**.
[36] N.Saikia, R.C.Deka; J.Mol.Model., **19**, 215 **(2013)**.
[37] N.Saikia, S.K.Pati, R.C.Deka; J.Appl.Nanosci., **2**, 389 **(2012)**.
[38] N.Saikia, R.C.Deka; J.Comput and Theor Chem., **964**, 257 **(2011)**.
[39] N.Saikia, R.C.Deka; J.Chem.Phys.Lett., **500**, 65 **(2010)**.
[40] M.J.Frisch, M.J.Frisch, G.W.Trucks, H.B.Schlegel, G.E.Scuseria, M.A.Robb, J.R.Cheeseman, G.Scalmani, V.Barone, B.Mennucci, G.A.Petersson, H.Nakatsuji, M.Caricato, X.Li, H.P.Hratchian, A.F.Izmaylov, J.Bloino, G.Zheng, J.L.Sonnenberg, M.Hada, M.Ehara, K.Toyota, R.Fukuda, J.Hasegawa, M.Ishida, T.Nakajima, Y.Honda, O.Kitao, H.Nakai, T.Vreven, J.A.Montgomery, Jr., J.E.Peralta, F.Ogliaro, M.Bearpark, J.J.Heyd, E.Brothers, K.N.Kudin, V.N.Staroverov, R.Kobayashi, J.Normand, K.Raghavachari, A.Rendell, J.C.Burant, S.S.Iyengar, J.Tomasi, M.Cossi, N.Rega, J.M.Millam, M.Klene, J.E.Knox, J.B.Cross, V.Bakken, C.Adamo, J.Jaramillo, R.Gomperts, R.E.Stratmann, O.Yazyev, A.J.Austin, R.Cammi, C.Pomelli, J.W.Ochterski, R.L.Martin, K.Morokuma, V.G.Zakrzewski, G.A.Voth, P.Salvador, J.J.Dannenberg, S.Dapprich, A.D.Daniels, E.O.Farkas, J.B.Foresman, J.V.Ortiz, J.Cioslowski, D.J.Fox; Gaussian 09 Revision A.02; Gaussian Inc.: Wallingford, CT, **(2009)**.
[41] Y.Zhao, N.E.Schultz, D.G.Truhlar; J.Chem.Theory Comput., **2**, 364 **(2006)**.
[42] S.F.Boys, F.Bernardi; J.Mol.Phys., **19**, 553 **(1970)**.
[43] R.F.W.Bader; Atoms in molecules, a quantum theory, Oxford University Press, New York, **(1990)**.
[44] M.Breneman, K.B.Wiberg; J.Comput.Chem., **11**, 361 **(1990)**.
[45] P.V.R.Schleyer, C.Maerker, A.Dransfeld, H.Jiao, N.J.R.V.E.Hommes; J.Am.Chem.Soc., **118**, 6317 **(1996)**.
[46] Z.Chen, C.S.Wannere, C.Corminboeuf, R.Puchta, P.V.R.Schleyer; J.Chem.Rev., **105**, 3842 **(2005)**.
[47] K.Wolinski, J.F.Hinto, P.Pulay; J.Am.Chem.Soc., **112**, 8251 **(1990)**.
[48] HyperChem® for Windows and NT, Hypercube, Inc., Publication HC50-00-04-00 October, **(1996)**.
[49] T.A.Koopmans; Physica., **1**, 104 **(1934)**.
[50] R.S.Mulliken; J.Chem.Phys.A, **2**, 782 **(1934)**.
[51] J.W.G.Bloom, S.E.Wheeler; J.Angew.Chem. Int.Ed., **50**, 7847 **(2011)**.